



Tipping the scales: how clinical assessment shapes the neural correlates of Parkinson's disease mild cognitive impairment

Ignacio Aracil-Bolaños^{1,2,3,4} · Frederic Sampedro^{3,4} · Juan Marín-Lahoz^{1,2,3,4} · Andrea Horta-Barba^{1,3,4} · Saül Martínez-Horta^{1,3,4} · José María González-de-Echávarri⁵ · Jesús Pérez-Pérez^{1,3,4} · Helena Bejr-Kasem^{1,3,4} · Berta Pascual-Sedano^{1,2,4} · Mariángeles Botí^{1,3,4} · Antonia Campolongo^{1,3,4} · Cristina Izquierdo^{1,3,4} · Alexandre Gironell^{1,3,4} · Beatriz Gómez-Ansón^{2,3,4,6} · Jaime Kulisevsky^{1,2,3,4} · Javier Pagonabarraga^{1,2,3,4}

Accepted: 15 August 2021 / Published online: 22 September 2021

© The Author(s), under exclusive licence to Springer Science+Business Media, LLC, part of Springer Nature 2021

Abstract

Mild cognitive impairment in Parkinson's disease (PD-MCI) is associated with consistent structural and functional brain changes. Whether different approaches for diagnosing PD-MCI are equivalent in their neural correlates is presently unknown. We aimed to profile the neuroimaging changes associated with the two endorsed methods of diagnosing PD-MCI. We recruited 53 consecutive non-demented PD patients and classified them as PD-MCI according to comprehensive neuropsychological examination as operationalized by the Movement Disorders Task Force. Voxel-based morphometry, cortical thickness, functional connectivity and graph theoretical measures were obtained on a 3-Tesla MRI scanner. 18 patients (32%) were classified as PD-MCI with Level-II criteria, 19 (33%) with the Parkinson's disease Cognitive Rating Scale (PD-CRS) and 32 (60%) with the Montreal Cognitive Assessment (MoCA) scale. Though regions of atrophy differed across classifications, reduced gray matter in the precuneus was found using both Level-II and PD-CRS classifications in PD-MCI patients. Patients diagnosed with the PD-CRS also showed extensive changes in cortical thickness, concurring with the MoCA in regions of the cingulate cortex, and again with Level-II regarding cortical thinning in the precuneus. Functional connectivity analysis found higher coherence within salience network regions of interest, and decreased anticorrelations between salience/central executive and default-mode networks in the PD-CRS classification for PD-MCI patients. Graph theoretical metrics showed a widespread decrease in node degree for the three classifications in PD-MCI, whereas betweenness centrality was increased in select nodes of the default mode network (DMN). Clinical and neuroimaging commonalities between the endorsed methods of cognitive assessment suggest a corresponding set of neural correlates in PD-MCI: loss of structural integrity in DMN structures, mainly the precuneus, and a loss of weighted connections in the salience network that might be counterbalanced by increased centrality in the DMN. Furthermore, the similarity of the results between exhaustive Level-II and screening Level-I tools might have practical implications in the search for neuroimaging biomarkers of cognitive impairment in Parkinson's disease.

Keywords Parkinson's disease · Salience network · Default mode network · Functional neuroimaging

Frederic Sampedro and Juan Marín-Lahoz contributed equally to this work.

✉ Jaime Kulisevsky
jkulisevsky@santpau.cat

✉ Javier Pagonabarraga
jpagonabarraga@santpau.cat

¹ Movement Disorders Unit, Neurology Department, Sant Pau Hospital, Mas Casanovas 90-08041, Barcelona, Spain

² Departament de Medicina, Universitat Autònoma de Barcelona (U.A.B.), Barcelona, Spain

³ Institut d'Investigacions Biomèdiques- Sant Pau (IIB-Sant Pau), Barcelona, Spain

⁴ Centro de Investigación en Red-Enfermedades Neurodegenerativas (CIBERNED), Madrid, Spain

⁵ Neurology Department, Sant Pau Hospital, Barcelona, Spain

⁶ Neuroradiology Unit, Sant Pau Hospital, Barcelona, Spain

Introduction

Formal neuropsychological assessment reveals mild cognitive impairment (MCI) in one out of every four non-demented patients with Parkinson's disease (PD) (Aarsland & Kurz, 2010; Litvan et al., 2011), a diagnosis that strongly predicts subsequent dementia (PDD) (Pedersen et al., 2013; Hoogland et al., 2017; Pigott et al., 2015). An accurate identification of PD patients at high risk of rapid cognitive decline is paramount to ensure adequate clinical care, including reliable prognostic information for individual and populations, as well as appropriate sample selection for upcoming trials targeting cognitive impairment.

To progress in the validation of MCI in PD as a clinical marker, criteria for PD-MCI have been standardized by the Movement Disorder Society (MDS) (Hoogland et al., 2017; Litvan et al., 2012). Accordingly, PD-MCI can be diagnosed either as level-I, by using recommended global cognitive instruments with appropriate psychometric validation in PD (Skorvanek et al., 2018; Hoogland et al., 2018) or as level-II, with a comprehensive examination using two neuropsychological tests for each of five cognitive domains (Litvan et al., 2012). The validity of the diagnosis of PD-MCI as a predictor of conversion to PDD, according to level-II criteria, has been recently established (Hoogland et al., 2017). However, the consistency and comparability for detecting cognitive decline between level I and level II diagnosis, and between different recommended level-I instruments (Skorvanek et al., 2018), is less known (Hoogland et al., 2018).

Despite methodological heterogeneities, the clinical diagnosis of cognitive deterioration and PD-MCI has been consistently associated to early structural and functional neuroimaging changes (Pagonabarraga et al., 2013; González-Redondo et al., 2014; Mak et al., 2015; Gasca-Salas et al., 2016; Gee et al., 2017). Given that clinical classification is a necessary first step in any neuroimaging study regarding cognition in PD, there is a need to evaluate the association between clinical assessment and the neural correlates of PD-MCI. In the present study we aimed to explore neuroimaging changes in a prospective sample of non-demented PD patients with PD-MCI at accepted per-domain level II testing, as well as using recommended Level-I scales Montreal Cognitive Assessment Scale (MoCA) and Parkinson's Disease-Cognitive Rating Scale (PD-CRS) (Skorvanek et al., 2018). We hypothesized that if level I and level II diagnosis of PD-MCI are equivalent, a common pattern of gray matter loss and network disruption should emerge.

Methods

Participants

Fifty-seven patients with early to mid-stage idiopathic PD regularly attending the Movement Disorders Outpatient

Unit and who were willing to participate in this study were prospectively recruited. Inclusion criteria were diagnosis of PD according to the United Kingdom PD Society Brain Bank (Hughes et al., 1992) and exclusion criteria were: 1) presence of dementia, according to the MDS-PDD Criteria (Emre et al., 2007); Hoehn & Yahr scale >III; 2) presence of any other significant psychiatric, neurological or unstable systemic comorbidities; 3) pathological MRI findings beyond mild white matter hyperintensities, or not compatible with PD in MRI FLAIR sequence; and 4) presence of head motion or other MRI artifacts. Two patients were excluded because of dementia, and two were excluded after reviewing MRI images for quality control.

Cognitive assessment

Patients were assessed using a battery of neuropsychological tests to achieve level I and level II classification. For level I diagnosis we employed the MoCA and the PD-CRS, both endorsed instruments by the MDS (Skorvanek et al., 2018). For the PD-CRS we adopted the cut-off score of <83 points (Fernández de Bobadilla et al., 2013). For the MoCA we employed the recommended cut-off score of <26, which has shown the best trade-off between sensitivity and specificity as a screening tool as measured by the Youden index (Dalrymple-Alford et al., 2010). We also explored a lower cut-off score of <24 points for the MoCA, which represents the optimal diagnostic value in the same study at the cost of lower sensitivity. For level II classification we administered a comprehensive neuropsychological battery that included two recommended neuropsychological tests per cognitive domain. Attention and working memory were assessed using the Digit Span Backward and Trail Making Test-A; executive dysfunction was measured using the Trail Making Test B and phonemic fluency; visuospatial function was determined by the Rey-Osterrieth complex figure-copy- (ROCFT) and the Visual Object and Space Perception Battery (VOSP) (number location); language function was evaluated using the Boston Naming Test and the Token Test; and memory function was assessed using the Free and Cued Selective Reminding Test (FCSRT) and the ROCFT According to established MDS-II criteria (Litvan et al., 2012), patients were classified as PD-MCI when they were 1.5 standard deviations (SD) below the Spanish normative data (Peña-Casanova et al., 2009) in two tests within a single cognitive domain, or in two tests within two different cognitive domains. Although the MDS-Task Force proposes a cut-off that ranges between 1 and 2 SD, we chose 1.5 SD as recommended by the MDS Study group for the Validation of Mild Cognitive Impairment in Parkinson Disease, which considers that impairment beyond 1.5 SDs represents

clinically meaningful decline (Hoogland et al., 2017), and because decline from this cut-off better detects the risk of conversion from PD-MCI to PDD (Wood et al., 2016). Finally, Depression and Anxiety were assessed using the Hospital Anxiety and Depression Scale (HADS).

MRI acquisition and preprocessing

All participants had available structural and resting-state functional MRI. T1-weighted scans were acquired in a 3 T Philips Achieva, and were performed using a dedicated axial T13D-magnetization-prepared rapid gradient-echo (T13D-MP-RAGE) MRI: Repetition time/Echo time (TR/TE) 500/50 milliseconds, flip-angle = 8°, field of view (FOV) = 23 cm, an in-plane resolution of 256 × 256 and 1-mm slice thickness. Resting-state BOLD images during 12 min were also obtained. (TR = 2000 ms, FOV 240 mm, voxel size 3 mm, TE = 30 ms, flip angle 78°).

MRI scan acquisition, preprocessing pipeline and analysis of voxel-based morphometry (VBM) and functional connectivity (FC) have been described in our previous work (Martinez-Horta et al., 2016; Aracil-Bolaños et al., 2019). Briefly, gray matter volume (GMV) imaging data were obtained from T1-weighted images using a voxel-based morphometry (VBM) approach in SPM12 (<http://www.fil.ion.ucl.ac.uk/spm/>). The original T1-MRI images were segmented to obtain their corresponding gray matter tissue probability maps. These maps were then spatially normalized into 2x2x2mm MNI space using DARTEL (Ashburner, 2007). Finally, an isotropic smoothing of 8 mm full-width at half maximum (FWHM) was applied.

Cortical thickness (Cth) analysis was performed using the FreeSurfer 6.0 software package (<https://surfer.nmr.mgh.harvard.edu/>). The procedure of cortical reconstruction of structural MRI images has been fully described elsewhere (Fischl & Dale, 2000). Briefly, white matter and pial surfaces were generated following image intensity gradients, from which a Cth measure was obtained for each vertex of the surface. On visual inspection, no major surface reconstruction errors were observed in our sample. Cth maps were transformed to fsaverage space and smoothed using a Gaussian kernel of 15 mm FWHM.

Functional imaging pre-processing was performed using CONN v14p software and its standard processing pipeline (described in depth in (Whitfield-Gabrieli & Nieto-Castanon, 2012)). Spatial preprocessing of functional volumes included realignment, normalization, and smoothing (8-mm FWHM Gaussian filter), using CONN default parameter choices. Anatomical volumes were segmented into gray matter, white matter, and CSF areas, and the resulting masks were eroded (one voxel erosion, isotropic 4-mm voxel size) to minimize partial volume effects. The temporal time series characterizing the estimated subject

motion (three-rotation and three translation parameters, plus another six parameters representing their first-order temporal derivatives), as well as the BOLD time series within the subject-specific white matter mask (ten PCA parameters) and CSF mask (ten PCA parameters), were used as temporal covariates and removed from the BOLD functional data using linear regression, and the resulting residual BOLD time series were band-pass filtered ($0.01 \text{ Hz} < f < 0.10 \text{ Hz}$). A random subset of 256 voxels (the same voxels across subjects and sessions) was used to compute the sample distribution of voxel-to-voxel BOLD signal correlation values separately for each subject and session, before and after removal of the defined temporal covariates. We did not employ global signal regression, since it can introduce artifactual biases, remove potentially meaningful neural components, and introduce confounding effects across populations (for more details, see (Aarsland & Kurz, 2010)). The entire matrix of ROI-to-ROI functional connectivity values (bivariate correlation measure) was computed for each subject using the set of functional brain networks described in the Shirer atlas (Shirer et al., 2012) and available at https://findlab.stanford.edu/functional_ROIs.html was introduced in CONN, focusing on the Default-Mode, Central Executive and Salience network regions of interest (ROI) as described in our previous work (Aracil-Bolaños et al., 2019). We calculated the between- and within-network connectivity of three large-scale cognitive networks-Default-Mode (DMN), Salience (SN) and Central Executive (CEN) networks- using built-in CONN scripts (*conn_withinbetweenROItest*) for each subject.

Finally, for graph theoretical analysis, network construction, graph metrics and statistical analysis were performed using Graphvar v2.01 (Kruschwitz et al., 2015). The adjacency matrices were constructed using a cost threshold of .15, which represented the most adequate trade-off between global and local efficiency in our sample and thus a good measure of small-worldness (see Supplementary material, Figure 4). We analyzed weighted node degree, betweenness centrality and local efficiency, widely accepted graph-theoretical metrics in brain networks (Filippi et al., 2013). Gephi v 0.92 was used for rendering purposes (Bastian et al., 2009).

Statistical analyses

For the VBM analysis, the resulting GMV images were entered into a voxelwise, second-level, two-sample t-test analysis between Parkinson's disease normal cognition (PD-NC) and PD-MCI patient groups to determine GMV differences. This statistical model included age, sex, Unified Parkinson's Disease Rating Scale part III (UPDRS III) and total intracranial volume (TIV) as covariates of no interest. Results were considered significant using a $p < 0.005$

uncorrected threshold commonly used in the structural neuroimaging literature (Watanabe et al., 2013; Goldman et al., 2014). The resulting statistical maps were represented in three-dimensional renders available in the MRIcron tool (Rorden et al., 2007). For Cth, Vertexwise data was introduced into a generalized linear model (GLM) to compare cognitive groups, using age, sex and UPDRS III as covariates. Results were considered significant using a $p < 0.005$ uncorrected threshold.

For the functional connectivity comparisons between the cognitive networks, we performed a two-sample T-test to compare the cognitive groups according to each scale using age, sex and UDPRS III scores as covariates of no interest. The results were considered significant using a $p < 0.05$ threshold. For graph theoretical metrics, the statistical analysis was performed with the built-in General Linear Model tool in Graphvar, using age, sex and UPDRS III as covariates of no interest, and permutation testing to control for multiple comparisons ($n = 10,000$) with a statistical threshold of $p < 0.05$.

Results

Clinic and sociodemographic data

Fifty-three patients with early-to-mid stages of PD were included (age 68.4 ± 7 years; disease duration 6.4 ± 3 years, MDS-UPDRS III 23.5 ± 9). Patients in our sample showed no significant anxiety or depression (HADS-A 3 ± 2.7 , HADS-D 3 ± 2.8). Eighteen patients (33%) were classified as PD-MCI using MDS level II criteria. Using level I

classification, 19 patients (35%) were classified as PD-MCI according to the PD-CRS and 32 patients (60%) according to the MoCA. Of note, an alternate cut-off score of < 24 points for the MoCA classified 18 patients as PD-MCI (30%). Differences in age, sex, education, disease duration, disease severity, and levodopa equivalent daily dose (LEDD) are shown in Table 1.

We also explored the agreement between the global scales and MDS level II criteria (Table 2). Data showed that while MoCA captured a large proportion of PD-MCI patients identified by level II criteria (77% sensitivity, versus 61% for the PD-CRS), it did so by accurately diagnosing less than 50% of PD-NC patients (48% specificity). The negative predictive values (NPV) of MoCA and PD-CRS compared to level II were similar (79% for the PD-CRS to 81% for the MoCA) but positive predictive value (PPV) was higher for the PD-CRS (57% to 43%). Using the alternate < 24 cut-off for the MoCA, specificity increased at the expense of decreased sensitivity (80% and 56% respectively) and predictive values compared to gold-standard level II approached but did not improve on the PD-CRS (PPV 56%, NPV 75%). Table 3 shows the number of subjects in which the global scales agree with Level-II assessment, and subdomain analysis, in which multidomain involvement was shown to be predominant in both level I classifications.

Voxel-based morphometry

PD-CRS and Level-II criteria showed overlapping areas of gray matter decrease in the precuneus region of the DMN in PD-MCI patients. For this statistical level, the PD-CRS

Table 1 Demographic data of the population according to the three neuropsychological classifications

Neuropsychological evaluation	PD-CRS		MOCA (26)		Level-II		MoCA (24)	
	PD-NC	PD-MCI	PD-NC	PD-MCI	PD-NC	PD-MCI	PD-NC	PD-MCI
Cognitive status	PD-NC	PD-MCI	PD-NC	PD-MCI	PD-NC	PD-MCI	PD-NC	PD-MCI
N (total, 53)	34	19	21	32	35	18	37	16
Age, y	65.8 ± 6.7 $p < 0.001$	73 ± 4.5	67.8 ± 6.3 $p = 0.64$	68.7 ± 7.2	67.5 ± 6.8 $P = 0.24$	69.9 ± 6.8	68.58 ± 6.43 $P = 0.77$	67.98 ± 7.96
Sex, % men	69% 24/34 $p = 0.11$	52% 10/19	66% 14/21 $p = 0.51$	62% 20/32	68% 24/35 $P = 0.87$	44% 8/18	69%, 25/37 $P = 0.6$	43%, 7/16
PD onset, y	6.4 ± 3 $P = 0.89$	6.3 ± 3.2	5.4 ± 2.34 $P = 0.06$	6.9 ± 3.3	6.5 ± 2.6 $P = 0.65$	6 ± 3.8	6.19 ± 2.60 $P = 0.51$	6.92 ± 3.95
Education, Y	13 ± 4.3 $P = 0.07$	11 ± 4.6	14 ± 4.6 $P = 0.07$	12 ± 4.2	13 ± 4.6 $P = 0.25$	12 ± 4	13 ± 4.60 $P = 0.08$	11 ± 3.9
MDS-UPDRS III	22.6 ± 10 $p < 0.001$	29 ± 7	22 ± 7 $P = 0.08$	25.9 ± 8.9	24.4 ± 8.4 $P = 0.61$	25.1 ± 8.1	23 ± 7.3 $p = 0.07$	28 ± 10.1
H&Y	1.9 ± 0.7 $p = 0.57$	2 ± 1	1.9 ± 0.2 $P = 0.51$	2 ± 0.2	1.9 ± 0.3 $P = 0.57$	2	1.9 ± 0.3 $P = 0.53$	$2 \pm$
LEDD	681 ± 363 $p = 0.31$	597 ± 237	544.2 ± 291.1 $p = 0.07$	689.4 ± 321.9	698 ± 303 $P = 0.15$	556.5 ± 331	632 ± 285 $p = 0.89$	620 ± 272

Table 2 Sensitivity, specificity and predictive values of the Level-I classifications according to Level-II gold standard

n=53	PD-CRS	MoCA 26	MoCA 24	Level-II
MCI prevalence.	19, 33%	32, 60%	16/53, 30%	18, 32%
Sensitivity.	11/18, 61.1%	14/18, 77.8%	9/16, 56%	N/A
Specificity.	27/35, 77.1%	17/35, 48%	28/35, 80%	N/A
Positive Predictive Value.	11/19, 57.1%	14/32, 43.8%	9/16, 56%	N/A
Negative Predictive Value.	27/34, 79.4%	17/21, 81%	28/37, 75%	N/A

showed additional reductions in gray matter located in the anterior cingulate cortex and bilateral temporal cortices, while level-II highlighted a loss of gray matter in bilateral superior frontal cortices. The MoCA showed a more restricted reduction of gray matter in the anterior cingulate cortex and right inferior temporal cortex. None of these areas overlapped with those found with the other two classifications (Fig. 1). For the alternate cut-off score of <24 points, the MoCA showed gray matter reductions in bilateral fusiform gyri and right inferior frontal gyrus (Supplementary material, Figure 2).

Cortical thickness

In cortical thickness maps (Fig. 2), level-II criteria showed isolated areas of cortical thinning in the left precuneus and right inferior frontal gyrus. The PD-CRS showed widespread and marked cortical thinning in relevant cognition related areas, with bilateral involvement of the temporo-parieto-occipital junction, posterior superior temporal gyrus, precuneus, orbitofrontal gyrus, and anterior, mid and posterior cingulate cortices. The MoCA showed less extensive cortical thinning, restricted to areas of the anterior and posterior cingulate cortex, and left temporo-occipito-parietal junction. Alternatively, a cut-off score of <24 points showed a similar pattern of cortical thinning highlighting more severe cortical thinning in anterior and posterior cingulate cortex, but also including the right precuneus (Supplementary material, Figure 3).

Functional connectivity

Comparing functional connectivity within and between networks, PD-CRS showed a distinct pattern of higher salience network connectivity in PD-NC patients, whereas the rest of the large-scale networks showed no differences between cognition groups. Across networks, PD-MCI patients showed higher coupling between the DMN and both SN and CEN, indicating lower anticorrelations between these normally antagonistic networks. None of these changes were significant for the MoCA (<26, <24) or level-II classification (Fig. 3). Details about the connectivity figures can be found in Supplementary material, Table 1.

Graph theory

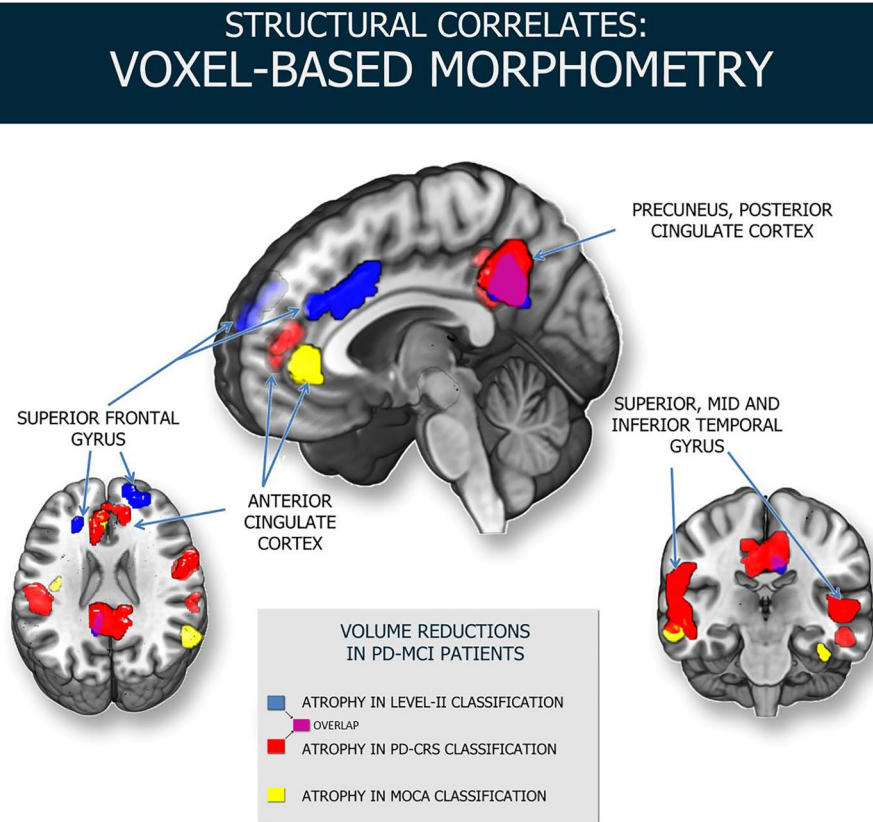
In graph theoretical analysis, the three classifications showed a lower weighted node degree in key nodes of the SN for the PD-MCI group (Fig. 4). Number and weight of connections were lower in the right supramarginal gyrus, mid frontal gyrus and the right anterior insula, whereas the posterior insula showed higher values in PD-MCI patients. Local efficiency was also lower in bilateral anterior insulae, mid frontal gyrus and right supramarginal gyrus, while PD-MCI patients showed an higher values in the mid cingulate cortex.

Weighted betweenness centrality was also found to be lower in the right mid frontal gyrus, but of note, some of the changes in centrality followed an opposing trend, with key nodes of the DMN showing higher centrality in

Table 3 Agreement between Level-I and gold-standard Level-II classifications methods in our sample

	PD-CRS	MoCA-26	MoCA-24	Level-II
MCI proportion in sample (53)	19/53 (33%)	32/53 (60%)	16/53 (30%)	18/53 (32%)
PD-NC, agreement with MDS-2, %	27/35, 77%	17/35, 48%	28/35, 80%	N/A
PD-MCI, agreement with MDS-2, %	11/18, 61%	14/18, 77%	9/16, 56%	N/A
Subdomain analysis	N=19	N=32	N=16	N=18
	- 8 (42%) did not meet criteria for MCI	- 18 (56%) did not meet criteria for MCI	- 6 (31%) did not meet criteria for PD-MCI.	- 17 (94%) multidomain MCI
	- 11 (59%) multidomain MCI	- 1 (4%) disexecutive MCI.	- 10 (62%) multidomain MCI.	- 1 (6%) disexecutive MCI.
		- 13 (40%) multidomain MCI.		

Fig. 1 Voxel-based morphometry showing structural correlates of the three cognitive classifications



MAIN FINDINGS

Overlapping volume decrease of the precuneus and posterior cingulate cortex in PD-CRS and Level-II criteria.
Volume reductions in anterior cingulate cortex in PD-CRS and MoCA classifications.

PD-MCI patients. A higher number of weighted shortest paths were found to cross the left and right precuneus in the PD-MCI group, thus showing higher centrality in these key nodes.

Detailed information about these metrics can be found in Supplementary material, Tables 2, 3 and 4.

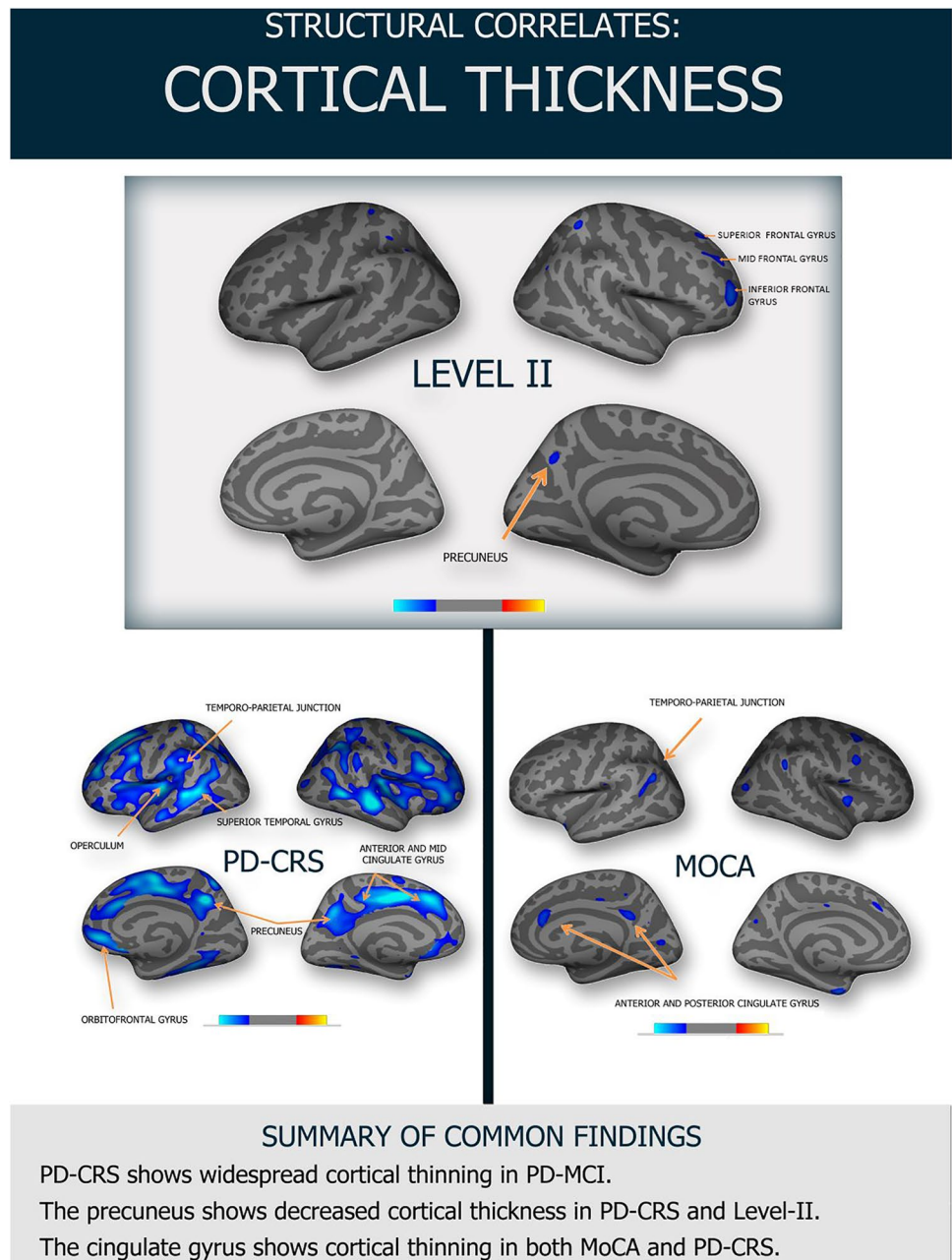
Discussion

In this study, we aimed to explore the neural correlates associated with the different accepted methods for diagnosing PD-MCI. Although differences were found between the gold-standard level II and the global scales in level I regarding patient classification and proportion of PD-MCI patients in the sample—as shown in Tables 1 and 2, these were expected given the intrinsic differences between the classification methods (Skorvanek et al., 2018). Far from intending

to outline which method produced the “best” correlates, we sought to investigate whether the diverse assessment tools converged in defining the structural and functional hallmarks of PD-MCI. To this effect, we have observed both commonalities and divergences in the neuroimaging findings associated with MDS recommended criteria.

On the structural analysis, both PD-CRS and MDS level II classifications showed overlapping loss of gray matter in the precuneus as a shared feature of PD-MCI, while the PD-CRS and the MoCA showed gray matter atrophy and cortical thinning in the anterior cingulate gyrus. While some studies have found no differences in cortical thickness in PD-MCI compared to PD-NC (Mak et al., 2014), our convergent findings replicate previous studies showing cortical thinning in the precuneus, supramarginal gyrus, and angular gyrus (Segura et al., 2014). The precuneus is a main component of the DMN (Greicius et al., 2003), one of the large-scale neurocognitive networks that has been shown to be a target

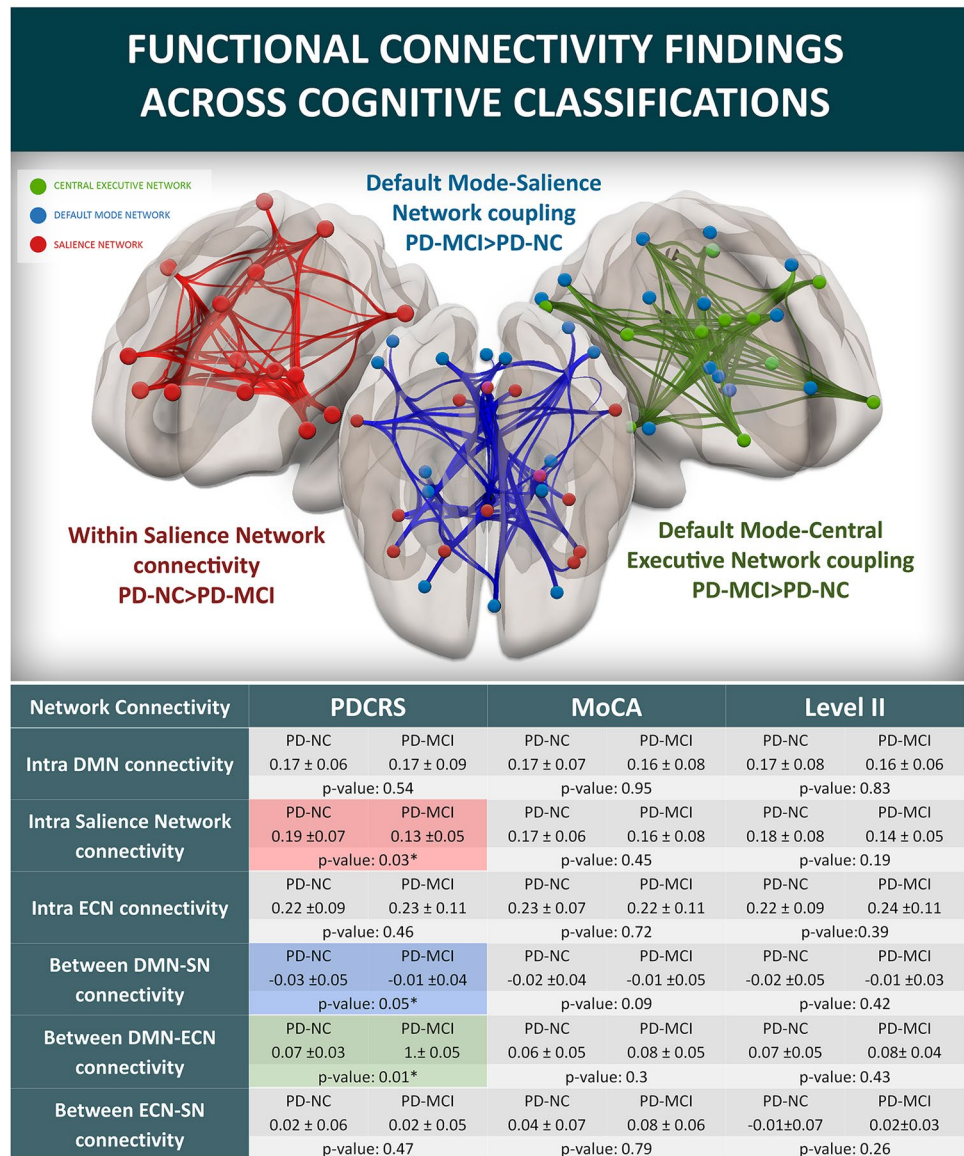
Fig. 2 Cortical thinning in PD-MCI compared to PD-NC patients according to level II, PD-CRS and MoCA



of a number of degenerative diseases (Seeley et al., 2009). In our sample, these changes are consistent between structural modalities, as the precuneus also showed cortical thinning in both level-II and PD-CRS classifications. The cortical thickness analysis showed that both level-I assessments highlighted the anterior cingulate cortex as a key affected area in the early stages of cognitive impairment. The dorsal anterior cingulate cortex is part of the salience network (Seeley et al., 2007) and as such it plays a pivotal role in the cognitive control of motor selection and execution (Hoffstaedter et al., 2014). To sum up, the three scales showed varying degrees of frontal disruption (superior frontal gyrus for the

Level-II classification, and anterior cingulate cortex for the Level-I classifications), but only the Level-I PD-CRS and the Level-II assessments captured both the anterior-executive and posterior cortical deficits that have been reported as neuropsychological hallmarks of the initial stages of PD-MCI (Kehagia et al., 2012; Pagonabarraga & Kulisevsky, 2012). For the MoCA, switching to a lower cut-off score might more closely resemble these findings, as gray matter loss was also found in posterior cortical regions such as the fusiform gyrus, and cortical thinning also involved the right precuneus. Of note, the structural changes disclosed by the PD-CRS were significantly more widespread, involving

Fig. 3 Functional connectivity findings across level I and level II assessment



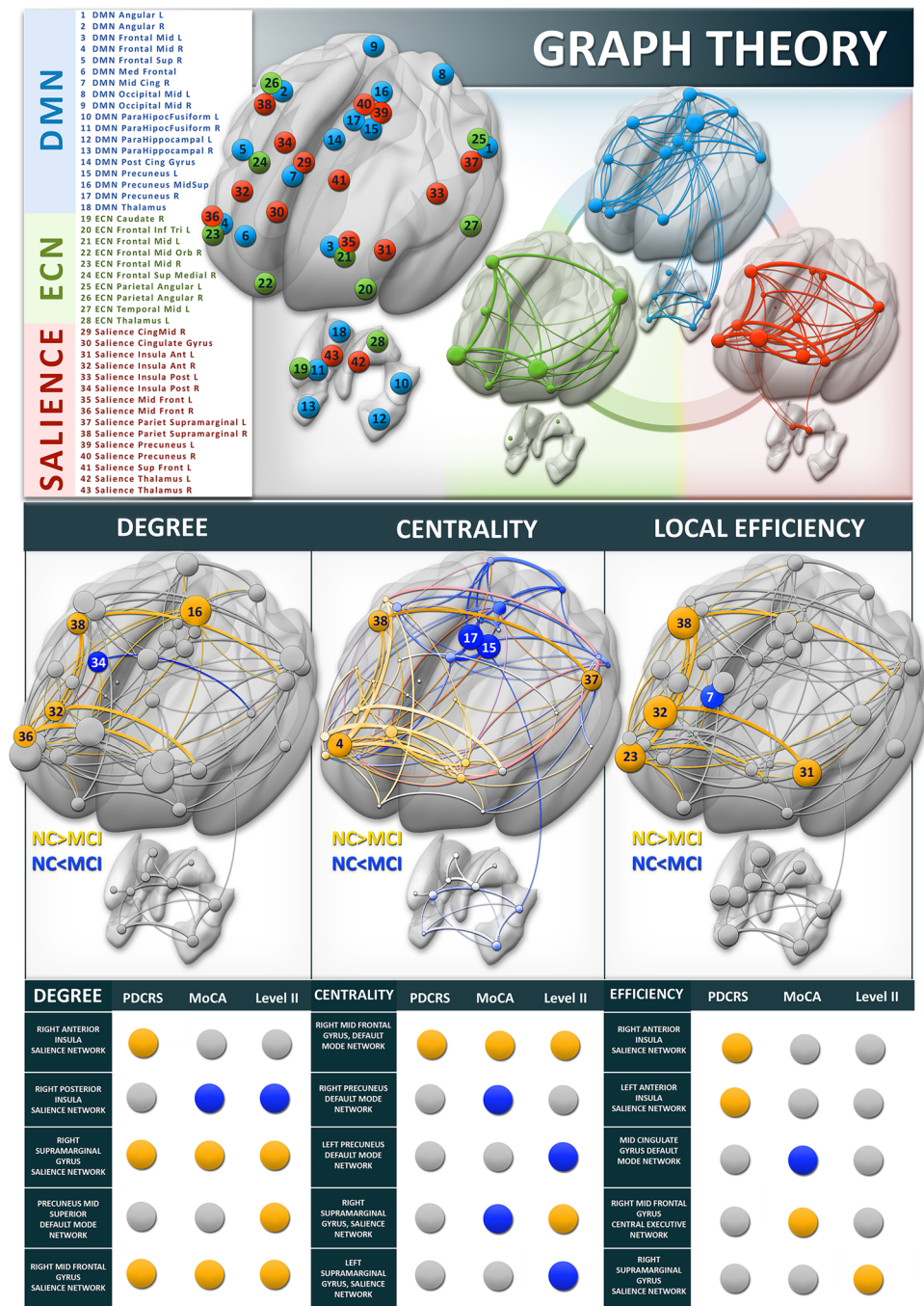
associative temporo-parietal areas previously reported as key cortical regions involved in the development of PD-MCI (Garcia-Diaz et al., 2014). These more extensive changes could be explained because although the PD-CRS and Level-II identify a similar proportion of PD-MCI cases in the sample, both assessments only concur in 61% of the patients.

Though tendencies emerge from the structural analyses, these findings suggest that there is still great heterogeneity among recommended cognitive scales and between different studies in PD cognition. This debate is part of an ongoing discussion in the neuroimaging community that ranges beyond PD (Darby et al., 2018), where similar diseases and symptoms seem to stem from the disruption of very different cortical areas. In our functional connectivity analysis, a decline in within-SN connectivity and decrease in normally-occurring anticorrelations between DMN and SN/CEN was

observed when using the PD-CRS classification. This lower connectivity in the frontoparietal regions of the salience network in early PD-MCI, as well as an increase in PD-NC, has been previously reported by our group and others (Aracil-Bolaños et al., 2019; Gorges et al., 2015; Christopher et al., 2015) These changes were not observed by the MoCA-at either cut-off score- or level II criteria, which stresses the impact that clinical classifications may have on the definition of neural correlates of PD-MCI, as well as in the search for imaging biomarkers.

The lack of agreement in functional connectivity, where only the PD-CRS showed a consistent alteration in between-network connectivity, contrasted with the results in graph theoretical metrics. Two key heteromodal nodes, the right anterior insula and the right supramarginal gyrus, showed a lower number and weight of connections in PD-MCI

Fig. 4 Graph-theoretical findings across level I and level II assessment



patients. The preferential disruption of highly associative areas has been previously described as a feature of the PD subtypes with greater cognitive impairment (Lopes et al., 2016). In particular, the disruption of the salience network seems to constitute a stepping stone in the path to cognitive decline, as previous studies have shown that the reduction in dopamine receptor availability signals the onset of mild cognitive impairment in PD (Christopher et al., 2015). Analysis of local efficiency confirmed a decrease in insular, frontal and supramarginal cortices in the different PD-MCI

classifications. Therefore, all the classification methods showed decreases in the node degree of salience network nodes, while changes in other large-scale networks were less apparent. Interestingly, previous works have found an increase in global efficiency and global clustering coefficient in PD-MCI patients associated with decreases in long-range connections (Baggio et al., 2014). Other studies, however, showed that PD-MCI progression contributed to a reduction in the functional segregation of cognitive networks (Lopes et al., 2016). In our model, local efficiency is preserved in

those regions that show higher weighted node degrees, and this coincidence in connection strength and organization could reflect compensation mechanisms that wane as disease progresses.

Of note, we also found regions of cognitive networks that show possible functional gains with the onset of cognitive decline. PD-MCI patients showed increases in the betweenness centrality of the precuneus, one of the main nodes of the posterior DMN, that is featured prominently in previous analyses of cognition and behaviour in PD (Lucas-Jiménez et al., 2016; Tessitore et al., 2012; Bejr-kasem et al., 2019). As the structural analysis proves, these areas that show higher centrality in our PD-MCI group are those affected by structural disruptions.

To sum up, two mechanisms of possible compensation are captured by different assessment scales. One seems to affect the node degree of the salience network and is present while patients remain cognitively “normal”, and the other appears in PD-MCI patients as an increase in the centrality of the posterior hubs of the DMN in the face of advancing grey matter loss. However, differences in the obtained neural correlates still persist. Across the three endorsed methods, PD-CRS seems to show the most consistent outline of widespread cortical volume and thickness decreases, coupled with functional connectivity disruptions that extend into architectural network features. These findings are not replicated by the other Level-I instrument, the MoCA, although lowering the cut-off score to 24 points does somewhat bridge the gap between this classification and the two other endorsed methods. The Level-II classification, although showing similar key features in structural precuneus volume loss and node degree decreases in the salience network, does not exhibit the same degree of consistency in the PD-MCI correlates. We believe that the use of different tests at the discretion on the researchers might hamper the ability of Level-II assessment to capture consistent PD-MCI correlates.

We acknowledge several limitations in this study. First, the study could be underpowered to detect differences and similarities in the diverse cognitive scales. Nevertheless, the proportion of patients classified as having PD-MCI using level II and PD-CRS is consistent with data from the literature (Litvan et al., 2011; Svenningsson et al., 2012). Second, an uncorrected statistical threshold was applied throughout the imaging analysis in order to capture changes across different modalities; although this is a threshold commonly employed in neuroimaging of movement disorders (Watanabe et al., 2013; Goldman et al., 2014) results should be considered exploratory. Third, longitudinal studies will be required to properly cement these findings. Strengths of the present work include the multimodal imaging approach that provides complementary evidences of structural and functional disruptions and the comprehensive

neuropsychological battery employed that allows for both level I and level II classification.

Conclusions

To sum up, neuroimaging traits that define PD-MCI emerge from both Level-I and Level-II with two relevant implications: first, our clinical classifications seem to reflect converging structural and functional changes in PD-MCI; and second, short assessment Level-I scales retain the ability to identify the neural correlates of the more time-consuming Level-II, although with some particularities.

Supplementary Information The online version contains supplementary material available at <https://doi.org/10.1007/s11682-021-00543-3>.

Author contributions Ignacio Aracil-Bolaños contributed to conception, organization and execution of the research project; designed and executed the imaging and statistical analyses and wrote the first draft.

Frederic Sampedro contributed to execution of the research project, assisted in statistical and imaging analyses and provided review and critique of the manuscript.

Juan Marín-Lahoz contributed to execution of the research project, assisted in statistical analysis and provided review and critique of the manuscript.

Andrea Horta-Barba contributed to conception and execution of the research project and provided review and critique of the manuscript.

Saül Martínez-Horta contributed to conception and execution of the research project and provided review and critique of the manuscript.

José María González-de-Echavarrri contributed to the execution of the research project and assisted in statistical and imaging analyses.

Mariángeles Botí contributed to conception and execution of the research project and provided review and critique of the manuscript.

Jesús Pérez-Pérez contributed to conception and execution of the research project and provided review and critique of the manuscript.

Helena Bejr-Kasem contributed to conception and execution of the research project and provided review and critique of the manuscript.

Berta Pascual-Sedano contributed to conception and execution of the research project and provided review and critique of the manuscript.

Antonia Campolongo contributed to organization and execution of the research project and provided review and critique of the manuscript.

Cristina Izquierdo contributed to organization and execution of the research project and provided review and critique of the manuscript.

Alexandre Gironell contributed to organization and execution of the research project and provided review and critique of the manuscript.

Beatriz Gómez-Ansón contributed to organization and execution of the research project and provided review and critique of the manuscript.

Jaime Kulisevsky contributed to conception, organization and execution of the research project and provided review and critique of the manuscript.

Javier Pagonabarraga contributed to conception, organization and execution of the research project and provided review and critique of the manuscript.

Funding The present work has received funding from

- La Marató de TV3, Expedient number 20142910

- FIS Grant PI14/02058, PI 18/01717.

- CIBERNED (Fundación CIEN, Instituto de Salud Carlos III, Spain)

Declarations

All patients provided written informed consent according to the Declaration of Helsinki. The study was approved by the Ethics Committee for Clinical Research at the Hospital de la Santa Creu i Sant Pau, Barcelona.

Conflict of interest The work of Dr. Aracil is supported by the Spanish Neurological Society via the Movement Disorders Study Group Grant, and is employed by Hospital de la Santa Creu i Sant Pau. The work of Dr. Bejr-Kasem is supported by Instituto de Salud Carlos III, Spain and has served on advisory or speakers' boards, and received honoraria from Zambon. Dr. Javier Pagonabarraga has served on advisory or speakers' boards, and received honoraria from UCB, Zambon, AbbVie, Italfarmaco, Allergan, Ipsen and Bial, and received grants from CIBERNED & FIS PI14/02058 (Spanish Government grants) and Fundació La Marató de TV3 20,142,910. Dr. Kulisevsky has received research grants from CIBERNED & FIS PI15/00962 (Spanish Government grants), and Fundació La Marató de TV3 20,142,410, and consulting fees or speaker honoraria from Zambon, Roche, Abbvie, Bial, UCB and Teva. Jesus Perez-Perez is employed as a Joan Rodes researcher (Spanish Government contract) and received grants from FIS (PI17/001885). Saul Martinez-Horta, Mariángeles Boti, Andrea Horta-Barba, Frederic Sampedro, Alexandre Gironell, Antonia Campolongo, Cristina Izquierdo, José María González-de-Echávarri and Juan Marín-Lahoz are employed by Hospital de la Santa Creu i Sant Pau and report no other conflict of interest or funding.

References

- Aarsland, D., & Kurz, M. W. (2010). The epidemiology of dementia associated with Parkinson disease. *Journal of the Neurological Sciences*, 289(1–2), 18–22
- Aracil-Bolaños, I., Sampedro, F., Marín-Lahoz, J., Horta-Barba, A., Martínez-Horta, S., Botí, M., et al. (2019). 40(11), 3233–3242
- Ashburner, J. (2007). A fast diffeomorphic image registration algorithm. *Neuroimage*, 38(1), 95–113
- Baggio, H., Sala-Illonch, R., Valldeoriola, F., Compta, Y. (2014). Functional brain networks and cognitive deficits in Parkinson's disease. *Human Brain Mapping*, 35(9), 4620–4634
- Bastian, M., Heymann, S., Jacomy, M. (2009) Gephi: An Open Source Software for Exploring and Manipulating Networks. In: Proceedings of the Third International ICWSM Conference
- Bejr-kasem, H., Pagonabarraga, J., Martínez-Horta, S., Sampedro, F., Marín-Lahoz, J., Horta-Barba, A., et al. (2019). Disruption of the default mode network and its intrinsic functional connectivity underlies minor hallucinations in Parkinson's disease. *Movement Disorders*, 34(1), 78–86
- Christopher, L., Duff-Canning, S., Koshimori, Y., Segura, B., Boileau, I., Chen, R., et al. (2015). Salience network and parahippocampal dopamine dysfunction in memory-impaired parkinson disease. *Annals of Neurology*, 77(2), 269–280
- Dalrymple-Alford, J. C., MacAskill, M. R., Nakas, C. T., Livingston, L., Graham, C., Crucian, G. P., et al. (2010). The MoCA: Well-suited screen for cognitive impairment in Parkinson disease. *Neurology*, 75(19), 1717–1725
- Darby, R. R., Joutsma, J., & Fox, M. D. (2018). Network localization of heterogeneous neuroimaging findings. *Brain*, 142(1), 70–79
- Emre, M., Aarsland, D., Brown, R., Burn, D.J., Duyckaerts, C., Mizuno, Y., et al. (2007). Clinical diagnostic criteria for dementia associated with Parkinson's disease. *Movement Disorders*, 22(12), 1689–1707
- Fernández de Bobadilla, R., Pagonabarraga, J., Martínez-Horta, S., Pascual-Sedano, B., Campolongo, A., & Kulisevsky, J. (2013). Parkinson's disease-cognitive rating scale: Psychometrics for mild cognitive impairment. *Movement Disorders*, 28(10), 1376–1383
- Filippi, M., van den Heuvel, M. P., Fornito, A., He, Y., Hulshoff Pol, H. E., Agosta, F., et al. (2013). Assessment of system dysfunction in the brain through MRI-based connectomics. *Lancet Neurology*, 12(12), 1189–1199
- Fischl, B., & Dale, A.M. (2000). Measuring the thickness of the human cerebral cortex from magnetic resonance images. *Proceedings of the National Academy of Sciences*, 97(20), 11050–11055
- García-Díaz, A. I., Segura, B., Baggio, H. C., Martí, M. J., Valldeoriola, F., Compta, Y., et al. (2014). Structural MRI correlates of the MMSE and pentagon copying test in Parkinson's disease. *Parkinsonism and Related Disorders*, 20(12), 1405–1410
- Gasca-Salas, C., Clavero, P., García-García, D., Obeso, J. A., & Rodríguez-Oroz, M. C. (2016). Significance of visual hallucinations and cerebral hypometabolism in the risk of dementia in Parkinson's disease patients with mild cognitive impairment. *Human Brain Mapping*, 37(3), 968–977
- Gee, M., Dukart, J., Draganski, B., Wayne Martin, W. R., Emery, D., & Camicioli, R. (2017). Regional volumetric change in Parkinson's disease with cognitive decline. *Journal of the Neurological Sciences*, 373, 88–94
- Goldman, J. G., Stebbins, G. T., Dinh, V., Bernard, B., Merkitich, D., Detolledo-Morrell, L., et al. (2014). Visuo-perceptive region atrophy independent of cognitive status in patients with Parkinson's disease with hallucinations. *Brain*, 137(3), 849–859
- González-Redondo, R., García-García, D., Clavero, P., Gasca-Salas, C., García-Eulate, R., Zubieta, J. L., et al. (2014). Grey matter hypometabolism and atrophy in Parkinson's disease with cognitive impairment: A two-step process. *Brain*, 137(8), 2356–2367
- Gorges, M., Müller, H., Lulé, D., Consortium, L., Pinkhardt, E. H., Ludolph, A. C., et al. (2015). Neurobiology of aging to rise and to fall : Functional connectivity in cognitively normal and cognitively impaired patients with Parkinson's disease. *Neurobiology of Aging*, 36(4), 1727–1735
- Greicius, M.D., Krasnow, B., Reiss, A.L., Menon, V. (2003). Functional connectivity in the resting brain : A network analysis of the default mode hypothesis. *Proceedings of the National Academy of Sciences*, 100(1), 253–258
- Hoffstaedter, F., Greffkes, C., Caspers, S., Roski, C., Palomero-Gallagher, N., Laird, A. R., et al. (2014). The role of anterior midcingulate cortex in cognitive motor control: Evidence from functional connectivity analyses. *Human Brain Mapping*, 35(6), 2741–2753
- Hoogland, J., Boel, J. A., de Bie, R. M. A., Gekus, R. B., Schmand, B. A., Dalrymple-Alford, J. C., et al. (2017). Mild cognitive impairment as a risk factor for Parkinson's disease dementia. *Movement Disorders*, 32(7), 1056–1065
- Hoogland, J., van Wanrooij, L. L., Boel, J. A., Goldman, J. G., Stebbins, G. T., Dalrymple-Alford, J. C., et al. (2018). Detecting mild cognitive deficits in Parkinson's disease: Comparison of neuropsychological tests. *Movement Disorders*, 33(11), 1750–1759
- Hughes, A. J., Daniel, S. E., Kilford, L., & Lees, A. J. (1992). Accuracy of clinical diagnosis of idiopathic Parkinson's disease : A clinico-pathological study of 100 cases. *Journal of Neurology, Neurosurgery, and Psychiatry*, 55, 181–184
- Kehagia, A. A., Barker, R. A., & Robbins, T. W. (2012). Cognitive impairment in Parkinson's disease: The dual syndrome hypothesis. *Neurodegenerative Diseases*, 11(2), 79–92
- Kruschwitz, J. D., List, D., Waller, L., Rubinov, M., & Walter, H. (2015). GraphVar: A user-friendly toolbox for comprehensive graph analyses of functional brain connectivity. *Journal of Neuroscience Methods*, 245, 107–115
- Litvan, I., Aarsland, D., Adler, C. H., Goldman, J. G., Kulisevsky, J., Mollenhauer, B., et al. (2011). MDS task force on mild cognitive

- impairment in Parkinson's disease: Critical review of PD-MCI. *Movement Disorders*, 26(10), 1814–1824
- Litvan, I., Goldman, J. G., Tröster, A. I., Ben, A., Weintraub, D., Petersen, R. C., et al. (2012). Diagnostic criteria for mild cognitive impairment in Parkinson's disease: Movement Disorder Society task force guidelines. *Movement Disorders*, 27(3), 349–356
- Lopes, R., Delmaire, C., Defebvre, L., Moonen, A.J., Duits, A.A., Hofman, P., et al. (2016). Cognitive phenotypes in Parkinson's disease differ in terms of brain-network organization and connectivity. *Human Brain Mapping*, 38(3), 1604–1621
- Lucas-Jiménez, O., Ojeda, N., Peña, J., Díez-Cirarda, M., Cabrera-Zubizarreta, A., Gómez-Esteban, J. C., Gómez-Beldarrain, M. Á., & Ibarretxe-Bilbao, N. (2016). Altered functional connectivity in the default mode network is associated with cognitive impairment and brain anatomical changes in Parkinson's disease. *Park Relat Disord*, 33, 58–64
- Mak, E., Bergsland, N., Dwyer, M. G., Zivadinov, R., & Kandiah, N. (2014). Subcortical atrophy is associated with cognitive impairment in mild Parkinson disease: A combined investigation of volumetric changes, cortical thickness, and vertex-based shape analysis. *AJNR. American Journal of Neuroradiology*, 35(12), 2257–2264
- Mak, E., Su, L., Williams, G. B., Firbank, M. J., Lawson, R. A., Yarnall, A. J., et al. (2015). Baseline and longitudinal grey matter changes in newly diagnosed Parkinson's disease: ICICLE-PD study. *Brain*, 138(10), 2974–2986
- Martinez-Horta, S., Sampedro, F., Pagonabarraga, J., Fernandez-Bobadilla, R., Marin-Lahoz, J., Riba, J., et al. (2016). Non-demented Parkinson's disease patients with apathy show decreased grey matter volume in key executive and reward-related nodes. *Brain Imaging and Behavior*, 11(5), 1334–1342
- Pagonabarraga, J., & Kulisevsky, J. (2012). Cognitive impairment and dementia in Parkinson's disease. *Neurobiology of Disease*, 46(3), 590–596
- Pagonabarraga, J., Pascual-Sedano, B., Campolongo, A., Kulisevsky, J. (2013). Parkinson's disease-cognitive rating scale: Psychometrics for mild cognitive impairment. 28(10), 1376–1383
- Pedersen, K. F., Larsen, J. P., Tysnes, O. B., & Alves, G. (2013). Prognosis of mild cognitive impairment in early Parkinson disease: The Norwegian ParkWest study. *JAMA Neurology*, 70(5), 580–586
- Peña-Casanova, J., Blesa, R., Aguilar, M., Gramunt-Fombuena, N., Gómez-Ansón, B., Oliva, R., et al. (2009). Spanish multicenter normative studies (NEURONORMA project): Methods and sample characteristics. *Archives of Clinical Neuropsychology*, 24(4), 307–319
- Pigott, K., Rick, J., Xie, S. X., et al. (2015). Longitudinal study of normal cognition in Parkinson disease. *Neurology*, 85(15), 1276–1282
- Rorden, C., Karnath, H. O., & Bonilha, L. (2007). Improving lesion-symptom mapping. *Journal of Cognitive Neuroscience*, 19(7), 1081–1088
- Seeley, W.W., Menon, V., Schatzberg, A.F., Keller, J., Glover, G.H., Kenna, H., et al. (2007). Dissociable intrinsic connectivity networks for salience processing and executive control. *The Journal of Neuroscience*, 27(9), 2349–2356
- Seeley, W. W., Crawford, R. K., Zhou, J., Miller, B. L., & Greicius, M. D. (2009). Neurodegenerative diseases target large-scale human brain networks. *Neuron*, 62(1), 42–52
- Segura, B., Baggio, H. C., Marti, M. J., Valldeoriola, F., Compta, Y., Garcia-Diaz, A. I., et al. (2014). Cortical thinning associated with mild cognitive impairment in Parkinson's disease. *Movement Disorders*, 29(12), 1495–1503
- Shirer, W. R., Ryali, S., Rykhlevskaia, E., Menon, V., & Greicius, M. D. (2012). Decoding subject-driven cognitive states with whole-brain connectivity patterns. *Cerebral Cortex*, 22(1), 158–165
- Skorvanek, M., Goldman, J. G., Jahanshahi, M., Marras, C., Rektorova, I., Schmand, B., et al. (2018). Global scales for cognitive screening in Parkinson's disease: Critique and recommendations. *Movement Disorders*, 33(2), 208–218
- Svenningsson, P., Westman, E., Ballard, C., & Aarsland, D. (2012). Cognitive impairment in patients with Parkinson's disease: Diagnosis, biomarkers, and treatment. *Lancet Neurology*, 11(8), 697–707
- Tessitore, A., Esposito, F., Vitale, C., Tessitore, A., Santangelo, G., Cirillo, G. (2012). Default-mode network connectivity in cognitively unimpaired patients with Parkinson disease. *Neurology*, 79(23), 2226–2232
- Watanabe, H., Senda, J., Kato, S., Ito, M., Atsuta, N., Hara, K., et al. (2013). Cortical and subcortical brain atrophy in Parkinson's disease with visual hallucination. *Movement Disorders*, 28(12), 1732–1736
- Whitfield-Gabrieli, S., & Nieto-Castanon, A. (2012). Conn: A functional connectivity toolbox for correlated and anticorrelated brain networks. *Brain Connectivity*, 2(3), 125–141
- Wood, K.-L., Myall, D. J., Livingston, L., Melzer, T. R., Pitcher, T. L., MacAskill, M. R., et al. (2016). Different PD-MCI criteria and risk of dementia in Parkinson's disease: 4-year longitudinal study. *Parkinson's Disease*, 2(1), 1–8

Publisher's note Springer Nature remains neutral with regard to jurisdictional claims in published maps and institutional affiliations.